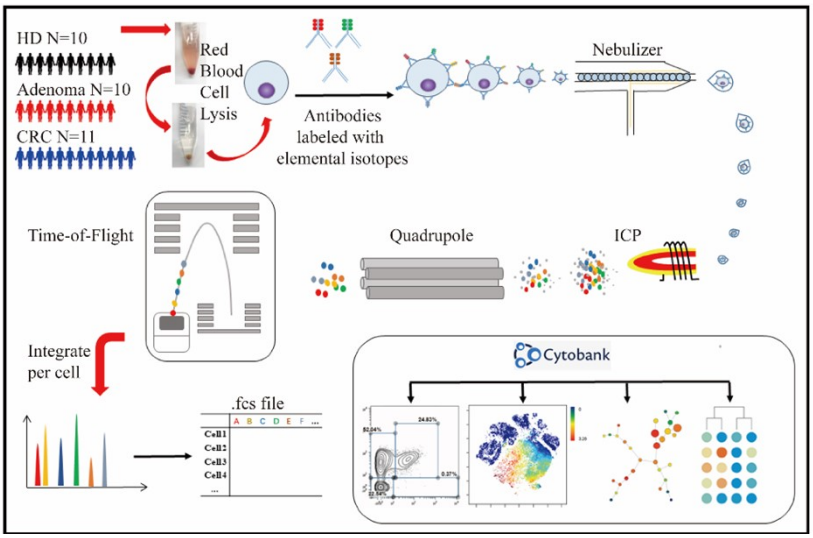

Fig S1 Schematic of mass cytometry analysis. Blood samples were collected from 10 healthy donors (HDs, N=10), 10 adenoma patients (Adenoma, N=10) and 11 colorectal cancer patients (CRC, N=11). Red blood cell lysis was performed in 4 hours after sample collection. Fixed cells were stained with metal-labeled antibodies. Then cells were passed in a single-cell suspension into the nebulizer and injected into ICP which could vaporize cells to ion clouds. The ion clouds entered the quadrupole filter to remove low-mass impurities. The remaining cloud of heavy metal ions were separated by mass-to-charge ratio across pushes of TOF. Mass signals of each channels were integrated in each cell and then recorded as .fcs files. Data was uploaded to Cytobank platform for further analysis.

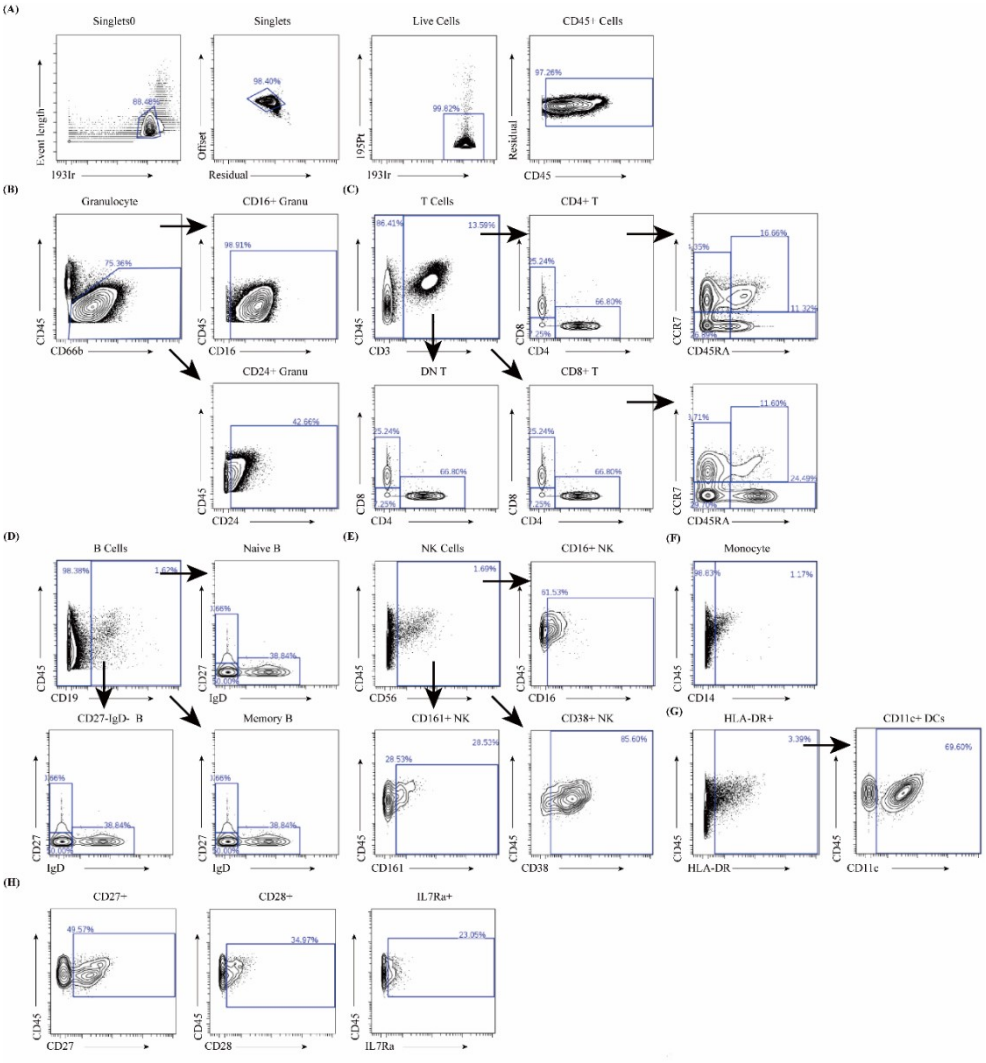

Fig S2 Gating strategy is shown for each population. Cell events for CRC sample are shown. Gates for all samples were applied based on the gating of CRC71. **(A)** $CD3^+$ T cells, $CD19^+$ B cells and $CD14^+$ Monocyte were excluded from $CD45^+$ Cells, and $CD66b^+CD45^+$ population was defined as Granulocyte. $CD24^+$ and $CD16^+$ Granulocyte were gated. **(B)** A singlet gate was drawn using event length by DNA (193Ir intercalator) to remove doublets and debris. Further gate on two Gaussian Discrimination parameters eliminates non-single cell events. Cisplatin was used to quantitatively discriminate live from dead cells. From the Live Cells gate, $CD45^+$ Cells were gated. **(C)** $CD19^+$ B cells were excluded from $CD45^+$ Cells, and $CD3^+CD45^+$ population was defined as T Cells. T Cells were further divided into $CD8^+$, $CD4^+$ and $CD8^-CD4^-$ populations. $CD8^+$ T Cells and $CD4^+$ T Cells were gated based on CD45RA and CD27: naïve (T_{naive}, $CD45RA^+CD27^+$), central memory (T_{cm}, $CD45RA^-CD27^+$), effector memory (T_{em}, $CD45RA^-CD27^-$), and terminally differentiated effector cells (T_{emra}, $CD45RA^+CD27^-$). **(D)** $CD3^+$ T cells and $CD14^+$ Monocyte were excluded from $CD45^+$ Cells, and $CD19^+CD45^+$ population was defined as B Cells. B Cells were separated based on expression of IgD and CD27 into three subsets: Naïve ($CD27^-IgD^+$), Memory ($CD27^+IgD^-$) and $CD27^-IgD^-$ B cells. **(E)** $CD3^+$ T cells, $CD19^+$ B cells and $CD14^+$ Monocyte were excluded from $CD45^+$ Cells, and $CD56^+CD45^+$ population was defined as NK Cells. $CD16^+$ NK Cells, $CD38^+$ NK Cells and $CD161^+$ NK Cells were identified. **(F)** $CD3^+$ T cells, and $CD19^+$ B cells were excluded from $CD45^+$ Cells, and $CD14^+CD45^+$ population was defined as Monocyte. **(G)** $CD3^+$ T cells, $CD19^+$ B cells and $CD14^+$ Monocyte were excluded from $CD45^+$ Cells, $HLA\text{-}DR^+$ was first gated and from which $CD11c^+CD45^+$ was defined as Myeloid DCs. **(H)** The portion of $CD27^+$, $CD28^+$ and $IL7Ra^+$ in $CD8^+$ T cells.

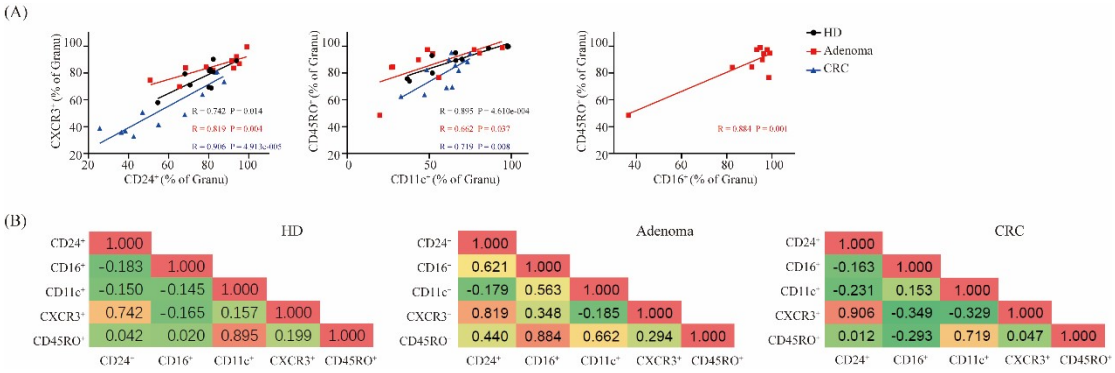

Fig S3 (A) Dot plots showing Pearson correlation coefficients for relationships between the frequencies of indicated cell populations (B) A heatmap showing the Pearson correlation coefficients for relationships between the frequencies of indicated cell populations.

Table S1 Characteristic features of study subjects.

Groups	HDs	Adenoma	CRC
Number	10	10	12
Age(years)	65.30(±1.27)	65.20(±3.19)	70.75(±7.78)
Gender(male : female)	0: 10	5:5	10:2
Location			
Left-sided hemicolon	-	5	4
Right-sided hemicolon	-	2	2
Rectum	-	-	4
Unknown	-	3	2
Histological			
Well/moderate	-	-	7
Poor/undifferentiated	-	-	2
Unknown	-	-	3

Note:

HDs: healthy donors;

Adenoma: adenoma patients;

CRC: Colorectal cancer patients;

Data is expressed as mean ± SD.

Unknown: Colonoscopy and pathology results didn't indicate the location in detail but only showed the presence of adenoma or cancer in the colorectal. Histological differentiation was not annotated in 3 cases of CRC.

Table S2 Antibodies used in panel A with the metal conjugate, clone and manufacturer.

Antigen	Conjugate	Clone	Manufacturer
CD45	89-Y	HI30	Fluidigm
CD196/CCR6	141-Pr	G034E3	Fluidigm
CD19	142-Nd	HIB19	Fluidigm
CD127/IL7-Ra	143-Nd	A019D5	Fluidigm
CD38	144-Nd	HIT2	Fluidigm
IgD	146-Nd	IA6-2	Fluidigm
CD11c	147-Sm	Bu15	Fluidigm
CD16	148-Nd	3G8	Fluidigm
CD194/CCR4	149-Sm	L291H4	Fluidigm
CD185/CXCR5	153-Eu	RF8B2	Fluidigm
CD3	154-Sm	UCHT1	Fluidigm
CD45RA	155-Gd	HI100	Fluidigm
CD27	158-Gd	L128	Fluidigm
CD28	160-Gd	CD28.2	Fluidigm
CD66b	162-Dy	80H3	Fluidigm
CD183/CXCR3	163-Dy	G025H7	Fluidigm
CD161	164-Dy	HP-3G10	Fluidigm
CD45RO	165-Ho	UCHL1	Fluidigm
CD24	166-Er	ML5	Fluidigm
CD197/CCR7	167-Er	G043H7	Fluidigm
CD8a	168-Er	SK1	Fluidigm
CD25	169-Tm	2A3	Fluidigm
CD20	171-Yb	2H7	Fluidigm
HLA-DR	173-Yb	L243	Fluidigm
CD4	174-Yb	SK3	Fluidigm
CD14	175-Lu	M5E2	Fluidigm
CD56	176-Yb	NCAM16.2	Fluidigm

Table S3 Immune cell types identified in Samples.

Cell Populations	Markers
Granulocyte	CD45+CD66b+CD3-CD19- CD14-
CD24+ Granu	CD45+CD66b+CD24+CD3-CD19- CD14-
CD16+ Granu	CD45+CD66b+CD161+CD3-CD19- CD14-
T cells	CD45+CD3+CD19- CD14-
CD8+ T cells	CD45+CD3+CD8+CD19- CD14-
Tnaive-like	CD45+CD3+CD8+CD45RA+CD27+CD19- CD14-
Tcm-like	CD45+CD3+CD8+CD45RA- CD27+CD19- CD14-
Tem-like	CD45+CD3+CD8+CD45RA- CD27-CD19- CD14-
Temra-like	CD45+CD3+CD8+CD45RA+ CD27-CD19- CD14-
CD4+ T cells	CD45+CD3+CD4+CD19- CD14-
Tnaive-like	CD45+CD3+CD4+CD45RA+CD27+CD19- CD14-
Tcm-like	CD45+CD3+CD4+CD45RA- CD27+CD19- CD14-
Tem-like	CD45+CD3+CD4+CD45RA- CD27-CD19- CD14-
Temra-like	CD45+CD3+CD4+CD45RA+ CD27-CD19- CD14-
CD8- CD4- T cells (DN)	CD45+CD3+ CD8-CD4-CD19- CD14-
B cells	CD45+CD19+CD3-CD14-
Naïve B cells	CD45+CD19+CD27-IgD+ CD3-CD14-
Memory B cells	CD45+CD19+CD27+IgD- CD3-CD14-
CD27-IgD- B cells	CD45+CD19+CD27-IgD- CD3-CD14-
NK cells	CD45+CD56+CD3-CD19- CD14-
CD16+ NK cells	CD45+CD56+CD16+CD3-CD19- CD14-
CD38+ NK cells	CD45+CD56+CD38+CD3-CD19- CD14-
CD161+ NK cells	CD45+CD56+CD161+CD3-CD19- CD14-
Monocyte	CD45+CD14+CD3-CD19-
CD11c+ DCs	CD45+HLADR+CD11c+CD3-CD19- CD14-